Energy Reports 7 (2021) 8378–8389

Contents lists available at ScienceDirect

Energy Reports

journal homepage: www.elsevier.com/locate/egyr

Simulation study on exhaust turbine power generation for waste heat recovery from exhaust of a diesel engine

Yongming Xu [a,*], Yimin Cui [b], Yaodong Wang [c], Peng Wang [a]

[a] School of Electrical and Information Engineering, Changzhou Institute of Technology, Changzhou, 213022, Jiangsu Province, China
[b] State Power Grid Shandong Anqiu City Power Supply Company, Anqiu, 262100, Shandong Province, China
[c] Department of Engineering, Durham University, Durham, DH1 3LE, UK

ARTICLE INFO

Article history:
Received 25 July 2021
Received in revised form 8 September 2021
Accepted 19 September 2021
Available online 7 October 2021

Keywords:
Exhaust turbine
Energy recovery
High-speed permanent magnet generator
Generator electromagnetic characteristics
System efficiency

ABSTRACT

Diesel engine has been used as the primary mover in vehicles for a long time. It is known that around 25%–30% of the fuel energy is wasted in the exhaust gas from diesel engines. In this study, a turbine power generation system including a 1.8 kW 60,000 r/min high-speed permanent magnet generator and a micro exhaust gas turbine, which is coupled to a diesel engine is designed and modeled to investigate its potential for recovering the wasted energy in the exhaust gas from a diesel engine. Computational models are set up using GT-POWER, MATLAB/SIMULINK and ANSOFT software. The performance and characteristics of the generator, the exhaust gas turbine and the engine are investigated. The simulation results showed that the exhaust turbine power generation system recovered the energy from the engine exhaust gas to generate electrical power. Simultaneously, the maximum power generated is 1.8 kW when the turbine speed is 60,000 rpm. The system efficiency reached its peak of 42.8% when the engine speed is 3000 rpm Last but not least, the electromagnetic characteristics of high-speed permanent magnet generator, which is coupled to an exhaust turbine, are also discussed and presented.

1. Introduction

In 2019, around 30% worldwide primary energy consumption is used for transportation, which is 122.45 quadrillion Btu (equals to 129.18 Exajoule (10^{18} J)), and the demand will increase 77% from 2018 to 2050 (U.S. Eenergy Information Administration (EIA), 2019). The major primary movers in transportation are mostly engines such as gas turbines for airplanes and big ships and petrol and diesel engines for vehicles and ships, which consume large quantities of petrol and diesel fuels. The increased usage of fossil fuels has resulted in huge amount of greenhouse gas emissions into the atmosphere, which has caused serious global warming and climate changes. Therefore, it is necessary to find solutions to reduce the consumptions of fossil fuels in transportation sector by increasing the energy conversion efficiency of the heat engines (Bin Mamat and Martinez-Botas, 2016). In the total energy released by fuel in the combustion process of engines, effective work output accounts for (20–45)% (Orr et al., 2016; Venkateswarlu and Suresh, 2018) and the rest of the energy is dissipated to the environment in the form of waste heat from exhaust gas and cooling system. The energy carried by exhaust gas accounts for about (28–44)% of the total fuel energy (Venkateswarlu and Suresh, 2018; Armstead and Miers, 2014). This is a huge resource of energy wasted, which may be recovered and utilized. Numerous studies have been carried out and some solutions have been found but they are not being widely used because of their disadvantages or limitations. These technological solutions can be categorized as following areas (Orr et al., 2016; Venkateswarlu and Suresh, 2018; Armstead and Miers, 2014; Arnaud et al., 2014): (a) organic Rankine cycle (ORC): the method use a cycle similar to the steam Rankine cycle but the working mediums are organic fluids such as different refrigerants (Venkateswarlu and Suresh, 2018; Nadaf and Gangavati, 2014); (b) turbocharging: the technology has been mainly used in diesel engines to boost the mass flow of intake air into engine cylinders by utilize the thermal energy in the exhaust gas to drive an exhaust gas turbine, which drives an air compressor to increase the air pressure into the cylinder (Romagnoli et al., 2017; Shu and Liang, 2013); (c) cogeneration/trigeneration: these technologies use the waste heat from the exhaust for heating and/or cooling through absorption or adsorption cooling cycles (Shu and Liang, 2013; Lin and Wang, 2007); (d) thermoelectric power generation: it uses waste heat to heat a thermoelectric module to generate electrical power (Orr et al., 2016; Nadaf and Gangavati, 2014). (e) use of power turbine to recover the energy in the exhaust gas and output mechanical power together with the engines, which is called as 'turbocompound engine'; or coupled

* Corresponding author.
E-mail address: xuyongming@czu.cn (Y. Xu).

https://doi.org/10.1016/j.egyr.2021.09.083

to an electrical power generator to generate electricity (Zhao et al., 2014). For ORC and cogeneration/trigeneration systems, their sizes are too big to be installed onto a vehicle, which limited their applications. Turbocharging has mainly been used for diesel engines but most them are used in big engines. The efficiency of thermoelectric module to generate electrical power has been proved to be of low efficiency.

Most recently, turbine-generator or turbo-generator for engine exhaust energy recovery has become a research hotspot because of its simple structure and small volume (Shu and Liang, 2013). But the challenge of turbine-generator is its high-speed, which can be between 10,000–100,000 r/min and it is difficult to design and manufacture a high-speed electrical generator and to couple to the turbine driven by exhaust gas. Zhao et al. (2014, 2015), Zhao and Li (2017) studied the influence of power turbine parameters, two-stage turbine interaction, steam injection on turbo-compound engine performance. They founded that reasonable combination of turbo-compound and steam injection can reduce fuel consumption rate by 6% to 11.2% at different speeds. Liu and Fu (2011) studied the energy flow distribution law of diesel exhaust turbocharging system and founded that about 13% of engine exhaust gas energy could be recovered by the turbo charger when it works at the high speed. Xie and He (2016) studied the influence of power turbine flow area, transmission ratio and turbocharged turbine flow area on the efficiency of a diesel engine in controllable mechanical turbo-compounding system, and the results showed that when 1600 r/min and 970 N m were the matching points, the flow area coefficient of a supercharged turbine was 0.875, the flow area coefficient of the power turbine was 1.6, fixed ratio was 25, the fuel consumption could be reduced by 4.3% and 1.28% under rated operating point and FTP-75 driving cycle. Dahl (2018) studied the control of exhaust gas recirculation valve, intake throttle valve and turbocharger wastegate in turbo-compound diesel engine and founded that compared with 'Proportional Integral Derivative' control scheme, 'Model Predictive Control' scheme reduced fuel consumption by 3%. In the above studies, the electromagnetic performance and power quality of the generator were not studied. Wei and Zhuge (2010) studied the system performance of three kinds of electric turbo-compounding systems: electrically assisted turbocharger, power turbine in series with the turbocharger, power turbine in parallel with the turbocharger. The results from their study showed that the performance of power turbine in parallel with the turbocharger system was improved by 4.0% under US06 driving cycle and 1.6% under FTP75 driving cycle. Xie and Li (2014) studied exhaust energy conversion efficiency and fuel saving effect of four turbo-compound systems. The results showed that electrically assisted turbocharger system could reduce the fuel consumption by 6.8% under the bus operating conditions and power turbine in series with the turbocharger system had the lowest fuel consumption, which could reduce fuel consumption by 5.1%. He and Xie (2017) studied the changes of engine specific fuel consumption and the key variables affecting the performance when using electric turbo-compounding for power generation by waste heat. The research showed that when the test speed was 1300 r/min, the cyclic injection quantity was 112 mg, and the isentropic efficiencies of charging turbine and the power turbine were 75%, the specific fuel consumption could be reduced to 182.5 g/(kW h). Li et al. (2014, 2015a,b), Xie et al. (2017) studied the control strategy of exhaust energy recovery system by using fuzzy control principle. The results showed that the turbine output power was smaller by using control strategy and the maximum recovery power of system could reach 1.7–1.9 kW under CYC-EUDC and CYC-US06-HWY driving cycles. Zhang (2014a,b, 2015a,b) carried out a series study on an EQ6100 internal combustion engine using turbine and generator in the exhaust gas system of the vehicle. The results showed that the turbine power was 8–9 kW, the average diameter was about 0.2445 m, and the optimal power of generator was 8 kW. Tang et al. (2016a,b) studied the transient performances of four modes including exhaust gas turbocharging (EGT), steam-assisted turbocharging (SAT), electronically controlled turbocharging (ECT) and supercharger-exhaust gas turbo-charging (SET). The results from their study showed that at the speed of 2000 r/min, compared with EGT, the specific fuel consumption of SET was decreased by 23.3%, while it could be reduced by 38.2% and 36.3% in SAT and ECT respectively. When a larger turbocharger was used, both the recovery efficiency of ECT and the utilization efficiency of exhaust energy increased at high speed and high load; and their maximum values reached up to 8.4% and 18.4% respectively. Ekberg and Eriksson (2017) studied the potential of using an electric turbocharger in a long haulage application. The results from the study showed that, by using an electric turbocharger and a charge sustainable control strategy, long haulage driving routes can be charge sustainable and consume less fuel than a conventional truck with fix turbine geometry; the fuel consumption could be reduced by 0.9%. Quinn and Dickinson (2005) added a power turbine to the exhaust pipe and driving a reluctance generator, and the exhaust energy of the engine was used to generate electricity. The results showed that fuel consumptions reduced by about 3% to 5% in engine driving cycles and up to 10% in individual conditions. The above studies mainly focused on mechanical and control. The interaction between the whole system (engine and turbine) and a generator was not investigated.

High-speed permanent magnet synchronous generators are mostly used in the waste heat recovery power generation system of automobile engines. At present, the permanent magnet generators do not integrate with the exhaust power turbine directly. Berardi and Bianchi (2017), Berardi et al. (2017), Berardi and Bianchi (2019) and Berardi et al. (2019) carried out a series study on the design of permanent magnet generator and the rotor loss calculation in an ORC system. The results showed that a dual three-phase winding solution allowed to achieve a lower flux density harmonic content and reduce rotor loss. Jung and Lee (2018) studied the design of an ultrahigh speed permanent magnet motor/generator driven at a rated output and speed of 10 kW and 70,000 r/min, respectively, for use in an electric-turbo compounding system. The results showed that the optimal design for the PM motor was using carbon fiber, which was not only reduced the eddy-current loss, but also ensured its structural safety. Gilson et al. (2017) and Gilson and Dubas (2016) studied the performance of different high-speed permanent magnet topologies and the noise problem of high-speed permanent magnet (HSPM) in electrically-assisted turbocharger (EAT) system. The results showed that compared with two 6-slot machines having different slot shapes, a slotless toroidally wound motor had higher efficiency and lower noise. Lim and Kim (2017) studied the design of 4 kW and 150krpm ultra-high-speed surface-mounted permanent-magnet synchronous motor (SPMSM) for an electrically assisted turbocharger. The results showed that the rising speed of the boost pressure exerted by the motor in the electrically assisted turbocharger was improved by about 44.9% over that of the conventional turbocharger. But this SPMSM cannot be used to recover the waste heat from the exhaust gas to generate electricity.

To sum up, the above studies on exhaust energy recovery system are mostly focused on the mechanical aspects of engines and power turbines. At present, few studies in the field of electrical machinery combined the generator and exhaust energy recovery system. Electromagnetic characteristics and the whole system performance of a high-speed permanent magnet generator coupled to an exhaust turbine power generation was

Table 1
Engine parameters.

Engine type	JX493ZLQ
Bore/mm	Φ93
Stroke/mm	102
Total displacement/L	2.771
Cylinder number	4
Compression ratio	17.2:1
Rated power	88 kW
Rated speed	3600 rpm

not investigated systematically. In view of the situation, this study investigates the electromagnetic characteristics of a high-speed permanent magnet generator connected to an exhaust turbine, which is driven by the exhaust gas from a 88 kW diesel engine; and the performance of the whole system integrated diesel engine, turbine and generator. The electromechanical coupling and performance matching between turbine, engine and the generator is the key factors to design the generator used for exhaust energy recovery system, so it is necessary to study the system comprehensive modeling and influence of diesel engine parameters on high-speed permanent magnet generator.

2. Methodology

2.1. Description of the system

The system of the exhaust turbine power generation (**ETPG**) is shown in Fig. 1. The system includes the following components: (1) a diesel engine with a turbocharger; (2) an ETPG generator, which composed of an exhaust power turbine and a high-speed permanent magnet generator (**HSPMG**). The HSPMG is an alternating current (**AC**) generator. The exhaust gas from diesel engine passes through the exhaust turbine in the ETPG and drives it running at high speed. The turbine drives the HSPMG to generate AC electricity. The AC is then converted to direct current (**DC**) by using a rectifier device and stored in a battery to realize the recovery of the waste heat (energy) in the exhaust gas. To carry out this simulation study, the sub-models of the system are described and set up in the following sections.

2.2. Engine submodel

The engine parameter is listed in Table 1. The engine model is made up of the inlet-and-exhaust system, injector, cylinder, crank train and turbo-charger based on GT-Power, as shown in Fig. 2. After calibration by the experimental data, the precision of the engine model is high enough for the following research, as shown in Fig. 3.

2.3. Power turbine sub-model

2.3.1. Mathematical model of power turbine

In the system, the power turbine is driven by high temperature and high-pressure exhaust gas and rotates at high speed. The power turbine converts the energy in the exhaust gas into mechanical energy; and drives the high-speed permanent magnet generator at high speed to generate electricity.

The working process of the power turbine can be described by the following formula (Xu, 2014):

$$m_{opt} = \psi^2 \left\{ 1 - \sqrt{\frac{\mu^2 \left(1-\varphi^2\right)\left(1-\cos^2\beta\psi^2\right)}{\cos^2\alpha_1\varphi^2 + \mu^2\left(1-\varphi^2\right)}} \right\} \tag{1}$$

$$U_{1opt} = \frac{\psi}{\sqrt{\mu^2\left(\frac{\cos^2\beta_2}{m_{opt}^2}\psi^2\right) + \frac{\cos^2\alpha_1\varphi^2\left(1-m_{opt}^2\psi^4\right)}{m_{opt}^2\psi^2\left(1-\varphi^2\right)}}} \tag{2}$$

Table 2
Main parameters of power turbine.

Engine type	H1A
Diameter/mm	60
Mass flow rate/kg/s	0.04–0.19
Max speed/rpm	57000

$$\lambda_{opt} = 1 - \left\{ \frac{\varphi U_{1opt}\cos\alpha_1\left(1-m_{opt}\psi^2\right)}{m_{opt}\psi^2\left(1-\varphi^2\right)} \right\}^2 \tag{3}$$

Where ψ is velocity loss coefficient of stator blade, φ is velocity loss coefficient of moving blade, μ is turbine radial degree, α_1 is the absolute outlet flow angle of stator blade, β_2 is the relative outlet flow angle of moving blade, m_{opt}, U_{1opt}, λ_{opt} is the optimal parameters of turbine efficiency maximization calculation; they are the key parameters which affect the turbine efficiency.

Ideal adiabatic velocity:

$$C_{ad} = \sqrt{\frac{2k}{k-1}RT_0\left[1-\left(\frac{p_2}{p_0}\right)^{\frac{k-1}{k}}\right] + C_0^2} \tag{4}$$

Where R is gas constant; T_0 is absolute temperature at inlet of turbine; C_0 is absolute velocity at inlet of turbine; p_0 is absolute pressure at inlet of turbine; p_2 is static pressure at outlet of turbine.

Peripheral velocity of turbine inlet outer diameter:

$$U_1 = U_{1pot}C_{ad} \tag{5}$$

Wheel work:

$$W_u = \frac{\left(c_1^2 - c_2^2\right) + \left(w_1^2 - w_2^2\right) + \left(U_1^2 - U_2^2\right)}{2} \tag{6}$$

Where c_1 is actual velocity at outlet of static blades; c_2 is absolute velocity at outlet of moving blades; w_1 is relative velocity at inlet of wheel; w_2 is actual relative velocity at outlet of moving blades.

Turbine power:

$$P_N = 0.001GW_u \tag{7}$$

Where G is exhaust gas flow.

Turbine inlet diameter:

$$D_1 = \frac{60U_1}{\pi n} \tag{8}$$

Where n is turbine working wheel speed.

Turbine outlet diameter:

$$D_2 = \mu D_1 \tag{9}$$

where μ is the turbine radial degree.

2.3.2. Sub-model for simulation of power turbine

The power turbine parameter is listed in Table 2. Based on the above equations, a simulation sub-model is set up in Simulink, as shown in Fig. 4. In Fig. 4, CO is the inlet velocity of exhaust gas into the turbine, and the exhaust velocity is obtained by the engine model as the value of CO.

2.4. High speed permanent magnet generator sub-model

In order to investigate the output voltage, output power and efficiency of HSPMG, a 2D simulation model of generator is established by Ansoft software, as shown in Fig. 5. The generator parameter is listed in Table 3.

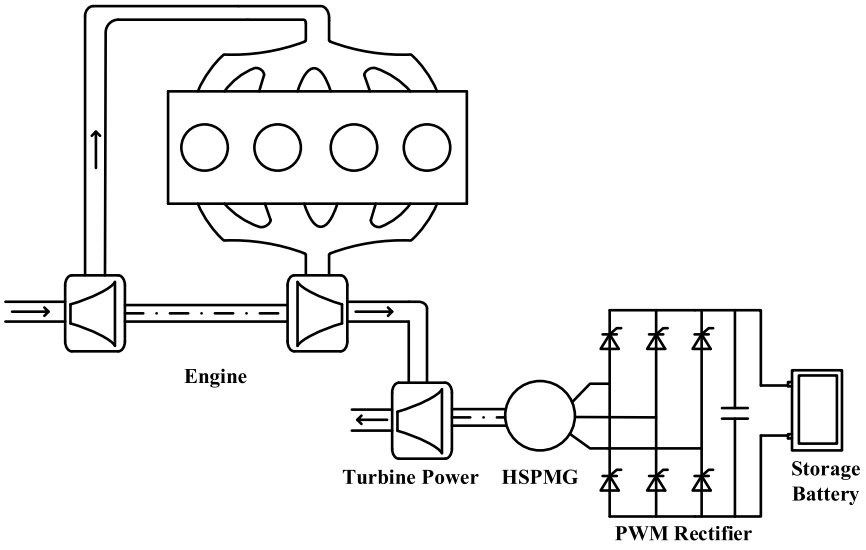

Fig. 1. Exhaust turbine power generation system.

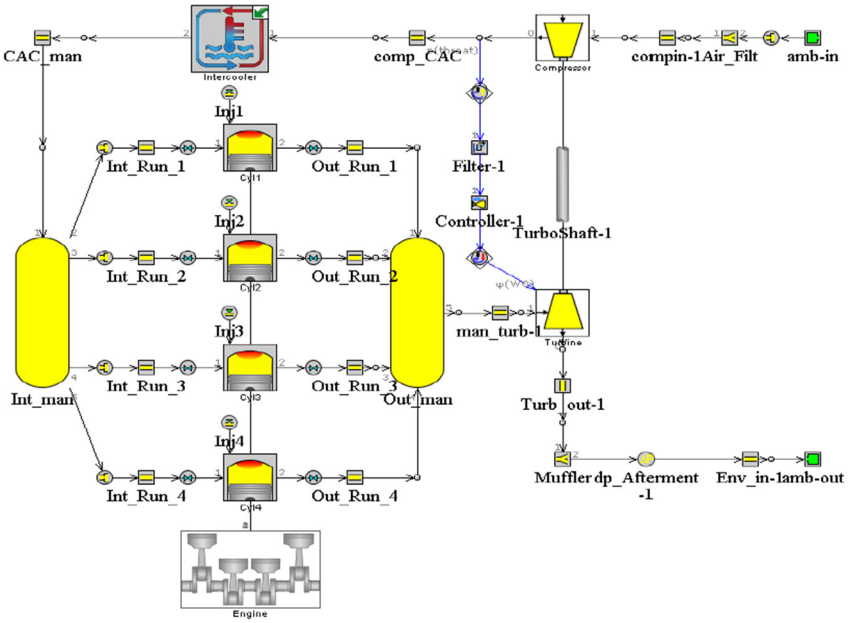

Fig. 2. Simulation model of the engine in GT-Power.

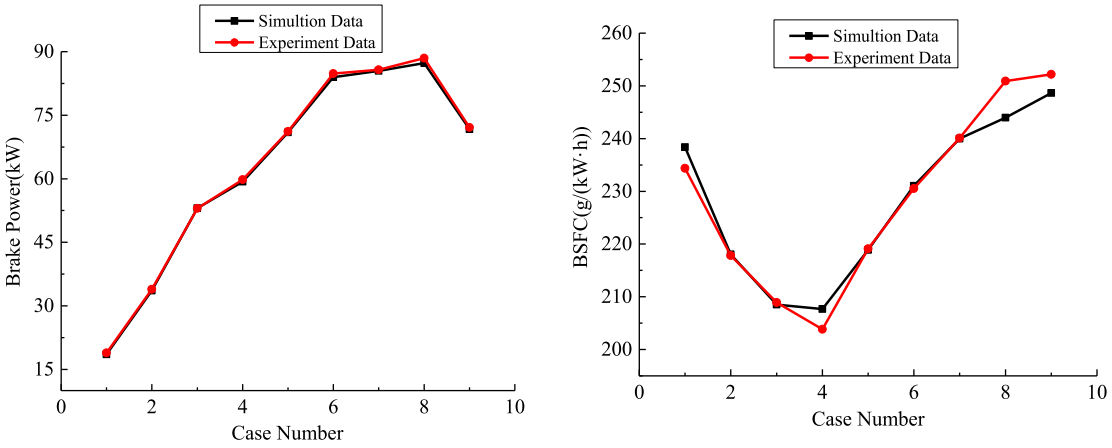

Fig. 3. The comparison of experimental and simulation results.

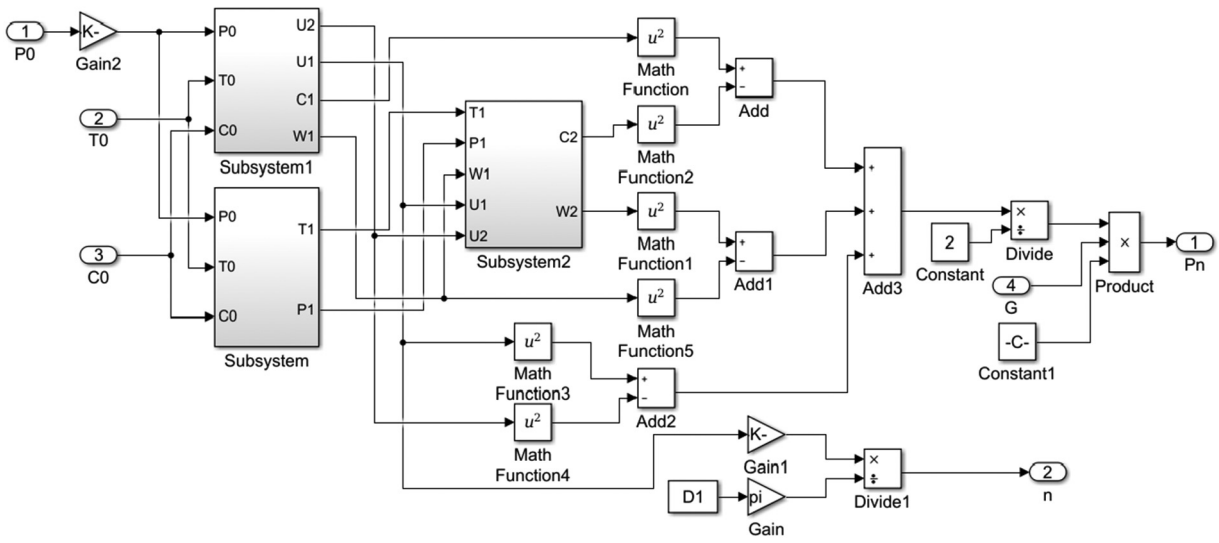

Fig. 4. Power turbine simulation model in Simulink.

Table 3
Main parameters of high-speed permanent magnet generator.

Generator parameters	Values
Rated power/kW	1.8
Rated voltage/V	80
Rated speed/rpm	60000
Pole pairs	1
Slot number	6
Core length/mm	43
Efficiency	>90%
Phase number	3

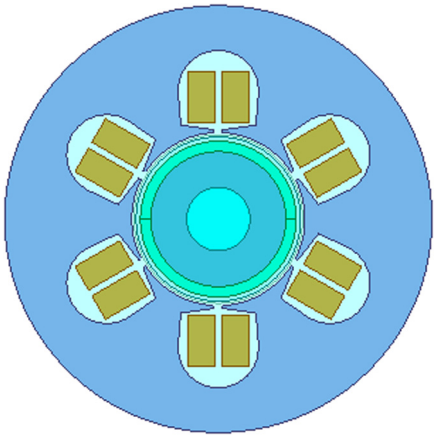

Fig. 5. High-speed permanent magnet synchronous generator model in Ansoft.

2.5. Integrated ETPG system model

The integrated ETPG system model is shown in Fig. 5. The system model includes two parts, as shown in Fig. 6 (a) and (b). The data such as pressure, temperature, mass flow and velocity output from the engine model can be transmitted to the power turbine sub-model in the Simulink, as shown in Fig. 6 (a). The speed data of the power turbine is stored in the workspace by 'To Workspace', and then the speed data is transmitted to the high-speed permanent magnet generator model by 'From Workspace' through Simplorer software, as shown in Fig. 6 (b).

3. Results and discussion

3.1. Turbo-generator characteristics

Fig. 7 reveals the relationship between the generated power and the turbo-generator speed. It is clear that the electrical power increases linearly as the speed increases. The power increases gradually from 5000 rpm to 60,000 rpm with a maximum power of 1.8 kW at 60,000 rpm.

In addition, the turbine power is investigated at different mass flow rates and speeds. The results are presented in Figs. 8 and 9. The power of the turbine increases linearly as the mass flow increases. As shown in Fig. 8, the maximum obtained power is 8.9 kW at 0.18 kg/s mass flow rate. Fig. 9 presents the variation of turbine power with turbine speed. As shown in Fig. 9, unlike mass flow rate, turbine power increases non-linearly along with the increase in the turbine speed with a maximum value of 7.4 kW at 52,000 rpm.

3.2. Influence of engine speed on turbine power generation system

3.2.1. The influence of engine speed on power turbine speed

The power turbine speed with time-variation at different engine speeds is shown in Fig. 10. It can be seen from Fig. 10, when the speed increases from 1800 r/min to 3600 r/min, the turbine speed also increases gradually. After 1 s, the speed range are 15240–27220 rpm, 31603–37826 rpm, 42426–48401 rpm and 48986–54274 r/min, respectively; and the frequency increases gradually. This is because, with the increase of engine speed, the flow rate of the exhaust gas, the exhaust temperature and pressure increase, that is, the energy (waste heat) flowing into the power turbine increases. So the turbine speed becomes higher.

3.2.2. The influence of speed on HSPMG

In order to study the influence of engine speed on voltage, output power and efficiency, the turbine speed curves under different engine speeds is transmitted to the high-speed permanent magnet generator model to obtain the electromagnetic characteristics of the HSPMG under different speeds, as shown in Figs. 11–14.

The influence of engine speed on peak voltage of generator is shown in Fig. 11. It can be seen from Fig. 11, the higher the engine speed is, the higher the peak voltage is. For example, as the load

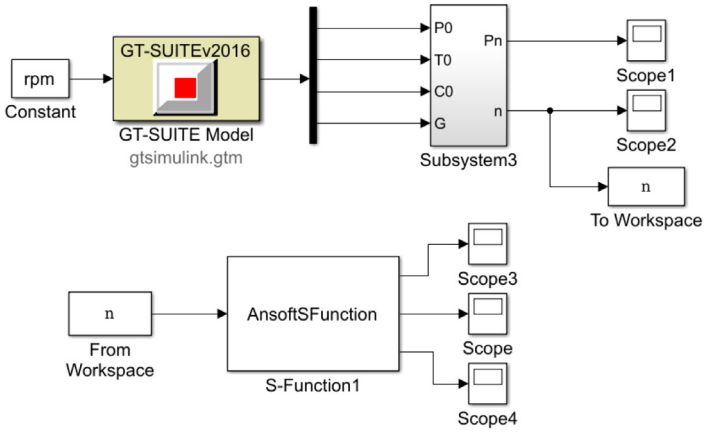

a)GT-Power and Simulink co-simulation model

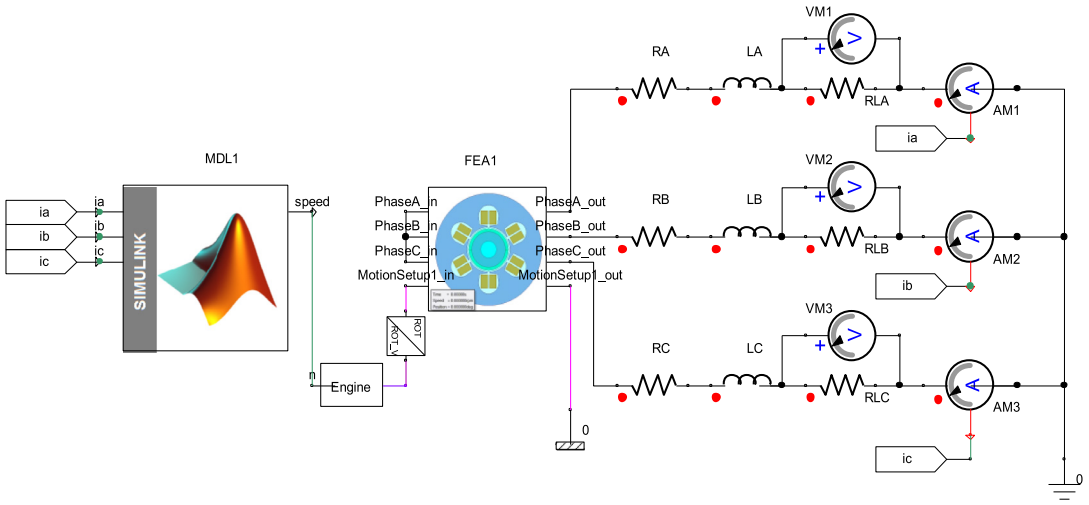

b)Simulink, Simplorer and Ansoft co-simulation model

Fig. 6. Integrated exhaust turbine power generation system model.

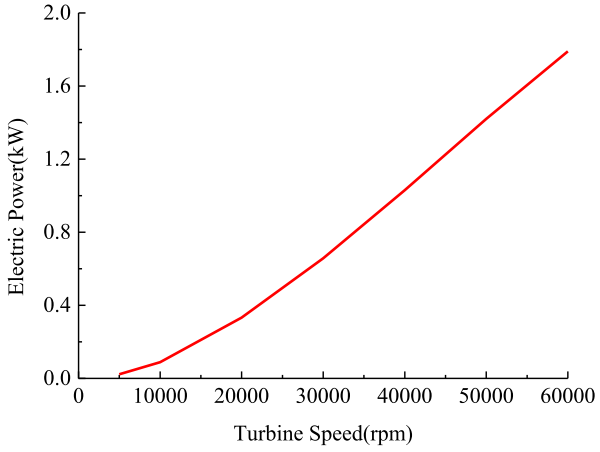

Fig. 7. Variation of power generation with speed.

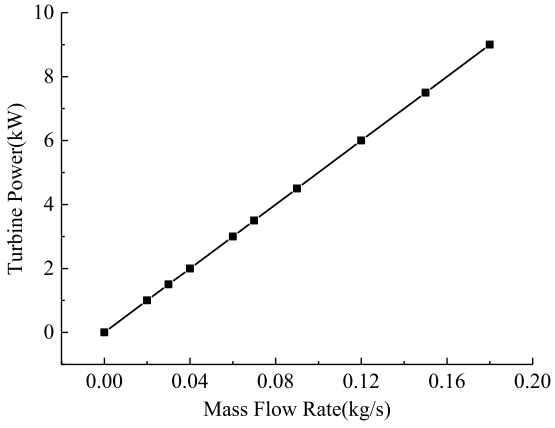

Fig. 8. Variation of power with mass flow rates.

is 2 Ω and the speed increases from 1800 rpm to 3600 rpm, the peak voltage of the generator increases from 33.8 V to 61.5 V.

The generator efficiency η can be calculated by the following formula:

$$\eta = \frac{U_A I_A + U_B I_B + U_C I_C}{U_A I_A + U_B I_B + U_C I_C + P_{loss}} \tag{10}$$

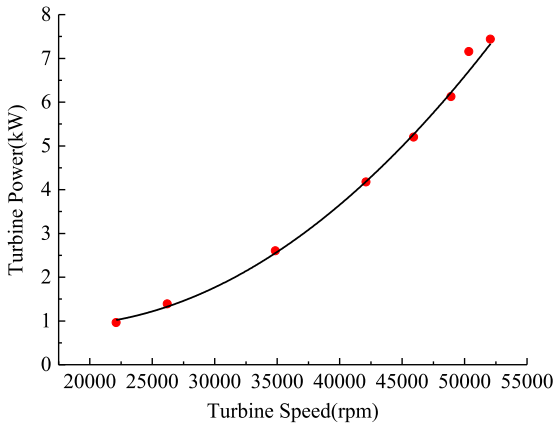

Fig. 9. Variation of power with turbine speed.

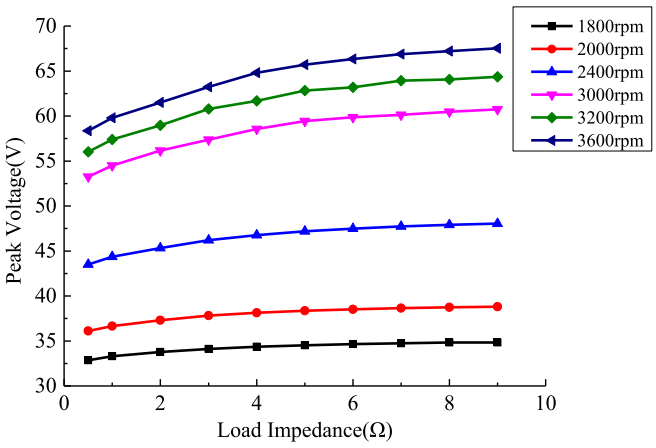

Fig. 11. The influence of engine speed on peak voltage of generator.

Where U_A, U_B, U_C are the phase voltage of each phase respectively; I_A, I_B, I_C are the phase current of each phase respectively, for generator the current depends on the load; P_{loss} is the total loss of generator.

The influence of engine speed on efficiency of generator is shown in Fig. 12. It can be seen from Fig. 12, under the same load condition, the higher the engine speed is, the higher the efficiency is. For example, when the load is 5 Ω and the speed is increased from 1800 rpm to 3600 rpm, the generator efficiency is increased from 93.1% to 95.8%.

Fig. 13 presents the influence of engine speed on output power of generator. As can be seen in Fig. 13, under the same load condition, the lower the engine speed is, the lower the output power is. For example, when the load is 5 Ω and the speed is reduced from 3600 rpm to 1800 rpm, the exhaust energy is reduced, and the speed of the generator coaxially connected with the power turbine is reduced, and the generator output power is reduced from 1.24 kW to 0.26 kW. The influence of engine speed on core loss of generator is shown in Fig. 14. It can be seen from Fig. 14, when the speed increases from 1800 rpm to 3600 rpm, the core loss increases gradually. For example, when the speed is 1800 rpm, the maximum core loss is 9.5 W; when the speed is 2400 rpm, the maximum core loss is 16.4 W.

3.3. Influence of fuel injection timing on turbine power generation system

3.3.1. The influence of fuel injection timing on power turbine speed

Fig. 15 presents the power turbine speed with time-variation under different fuel injection timings at 3600 rpm. It can be seen from Fig. 15, the turbine speed fluctuates steadily within a certain range after 0.6 s. When the injection timing is decreased from −8 deg to −5 deg, the maximum turbine speed is increased from 54164 r/min to 54763 r/min and the frequency is kept the same. This is because with the decrease of injection timing, the exhaust temperature and pressure gradually increase, and then the energy flowing into the power turbine increases. So the turbine speed becomes higher.

3.3.2. The influence of injection timing on generator

The influence of injection timing on peak voltage and effective current of generator is shown in Fig. 16. It can be seen from Fig. 16, when the fuel injection timing decreases from −9.93 deg to −5.93 deg, the peak voltage increases from 61.32 V to 62 V; and the effective current increases from 7.61 A to 7.66 A. The reason is that when the load is constant, as injection timing decreases, the exhaust energy increases, the generator speed increases accordingly which leads to the increase of output voltage and current from the generator. The influence of injection timing on power, core loss and efficiency of generator is shown in Fig. 17. It can be seen from Fig. 17, when the fuel injection

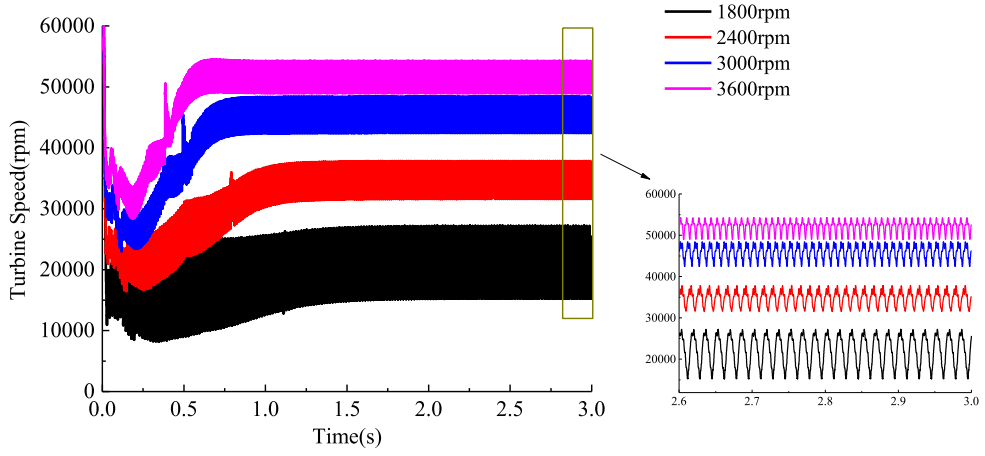

Fig. 10. The power turbine speed with time-variation at different engine speeds.

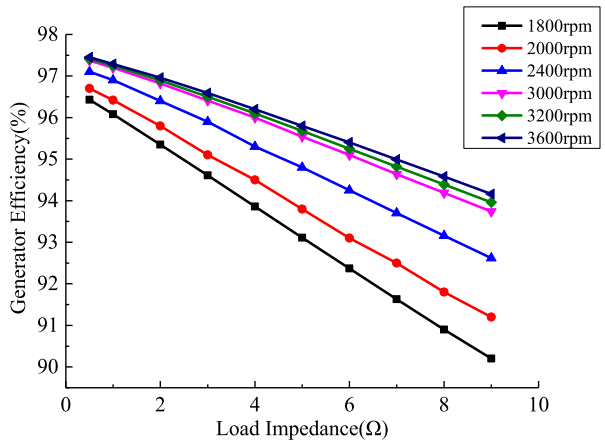

Fig. 12. The influence of engine speed on efficiency of generator.

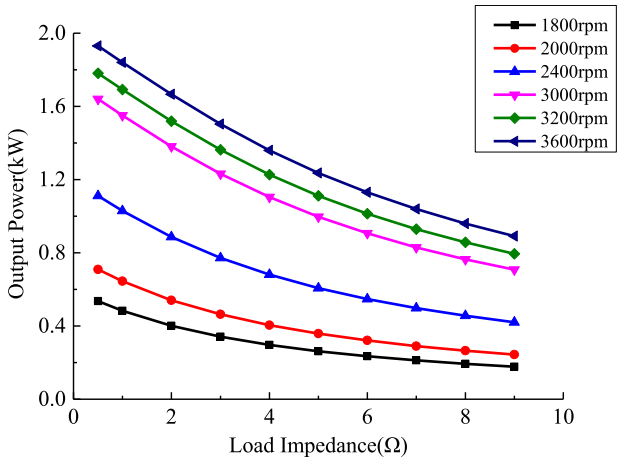

Fig. 13. The influence of engine speed on output power of generator.

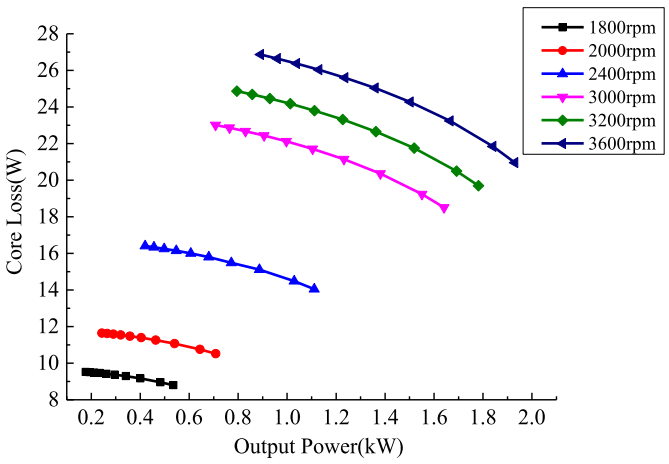

Fig. 14. The influence of engine speed on core loss of generator.

timing decreases from −9.93 deg to −5.93 deg, the output power increases from 1662 W to 1685 W; the core loss increases from 23.18 W to 23.43 W, and the efficiency increase is insignificant.

The generator frequency increases with the increase of its speed, and the iron loss is proportional to the frequency, so the iron loss will increase. But the increase is small, so the change of generator efficiency is not obvious.

The *THDu* of generator can be calculated by the following formula:

$$THDu = \frac{\sqrt{U_2^2 + U_3^2 + U_4^2 + \cdots + U_n^2}}{U_1} \times 100\% \tag{11}$$

Where *THDu* is the total harmonic distortion of voltage; U_1 is the effective value of fundamental voltage; U_n is the effective value of the *n*th harmonic voltage.

Fig. 18 presents the influence of injection timing on *THDu* of generator. It can be seen from Fig. 18, when the fuel injection timing decreases from −9.93 deg to −5.93 deg, the *THDu* increases from 0.032 to 0.09. The change of fuel injection advance angle will lead to the change of diesel engine exhaust energy, and then the generator speed will fluctuate in different range, and the electromagnetic performance of the generator will also change. When the fuel injection advance angle becomes smaller, the exhaust gas energy flowing into the turbine and the generator speed increase. The output voltage, current power also increase. *THDu* is the effective value of voltage fundamental wave and harmonics obtained through Fourier decomposition, which can be calculated by Eq. (11). The higher the rotational speed, the greater the *THDu*.

3.4. Influence of compression ratio on turbine power generation system

3.4.1. The influence of compression ratio on the speed of power turbine

The power turbine speed is investigated at different compression ratios. The results are presented in Fig. 19. It can be seen in Fig. 19, the turbine speed fluctuates steadily within a certain range after 0.6 s. When the compression ratio is increased from 14.2 to 18.2, the maximum turbine speed is decreased from 56,027 rpm to 53,762 rpm. The reason is that with the increase of the compression ratio, the exhaust temperature and pressure decreases gradually; the energy contained in the exhaust gas flowing into the power turbine decreases, so the turbine speed decreases.

3.4.2. The influence of compression ratio on the performance of generator

The peak voltage and effective current are investigated at different compression ratios can be seen in Fig. 20. As shown in Fig. 20, both lines have the same trend where the peak voltage and current decreases as the compression ratio increases. When the compression ratio is increased from 14.2 to 19.2, the peak voltage is decreased from 63.15 V to 60.62 V, the effective current is decreased from 7.75 V to 7.54 V. The power and core loss of the generator are investigated with compression ratio as depicted in Fig. 21. It is clear that the output power and core loss decreases as compression ratio increases. As the compression ratio increases from 14.2 to 19.2, the output power decreases from 1736 W to 1627 W, the core loss decreases from 23.95 W to 22.84 W.

The influence of compression ratio on efficiency and *THDu* of generator is shown in Fig. 22. It can be seen from Fig. 22, the lower the compression ratio is, the more efficiency and *THDu* of generator are obtained. As the compression ratio decreases from 19.2 to 14.2, the *THDu* increases from 0.023 to 0.078. The efficiency increases with increasing the compression ratio until it reaches its peak of 96.99% at 14.2 compression ratio.

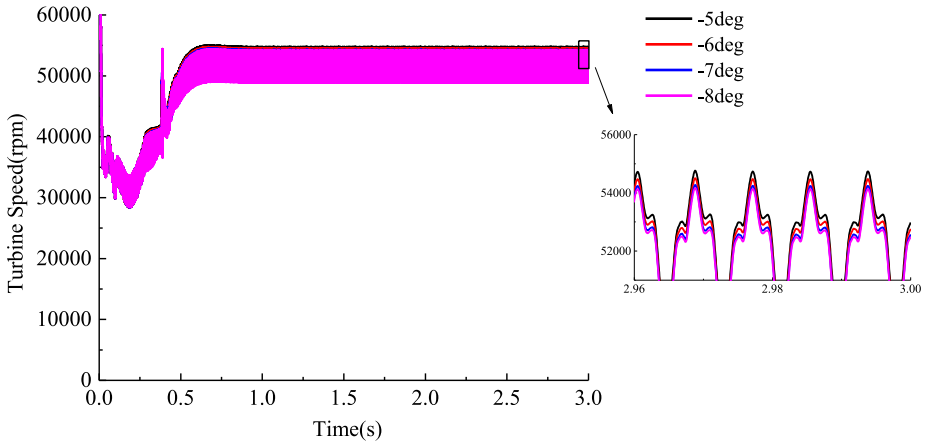

Fig. 15. The power turbine speed with time-variation at different injection timings.

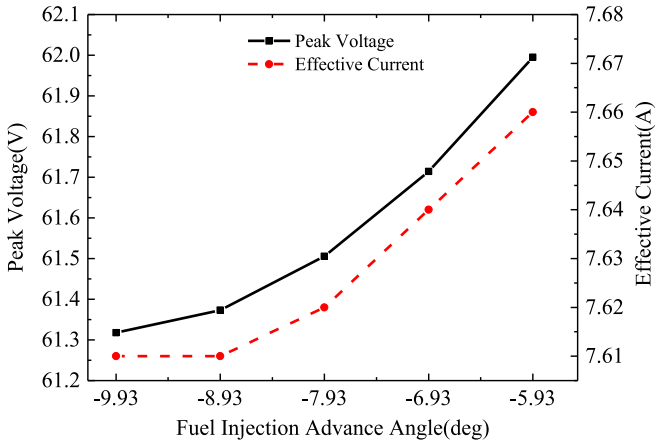

Fig. 16. The influence of injection timing on voltage and current of generator.

3.5. The efficiency of the system

The efficiency of exhaust turbine power generation system can be calculated by the following formula:

$$\eta_{sys} = \frac{P_e + P_t + P_g}{m_e H_u} \tag{12}$$

Where P_e is the effective power of engine, P_t is the output power of power turbine, P_g is the output power of generator, m_e is the fuel mass consumed by the system in unit time, H_u is the fuel calorific value.

Fig. 23 shows the relation of the system efficiency with the engine speed. It can be found that from Fig. 23, as the engine speed increases from 1800 r/min to 3000 r/min, the system efficiency increases gradually. The system efficiency then decreases gradually from 3000 rpm to 3600 rpm with a maximum efficiency of 42.8% at 3000 rpm.

Fig. 24 shows the system efficiency comparison of this research with the dual loop ORC systems (Giampieria et al., 2020), the combined heat and power generation (CHP), the Rankine cycle (RC), the transcritical Rankine cycle (TRC), the trilateral flash cycle (TFC) and the single flash cycle (SFC) (Rijpkema et al., 2017), and thermoelectric generation Alshammari et al. (2018). It should be noted that the efficiency in the figure is only for a certain research case, which may be different for different research objects.

It can been found from Fig. 4 that the system efficiency of dual loop ORC and CHP can be up to 90% and 70% respectively and higher than that of the others, including proposed method in this research. However, complex structure and larger volume of dual loop ORC and CHP are not suitable to be installed in the vehicle. For the remaining forms, the efficiency of the exhaust power turbine generation system is obviously higher than the others. The exhaust power turbine generation system for energy recovery

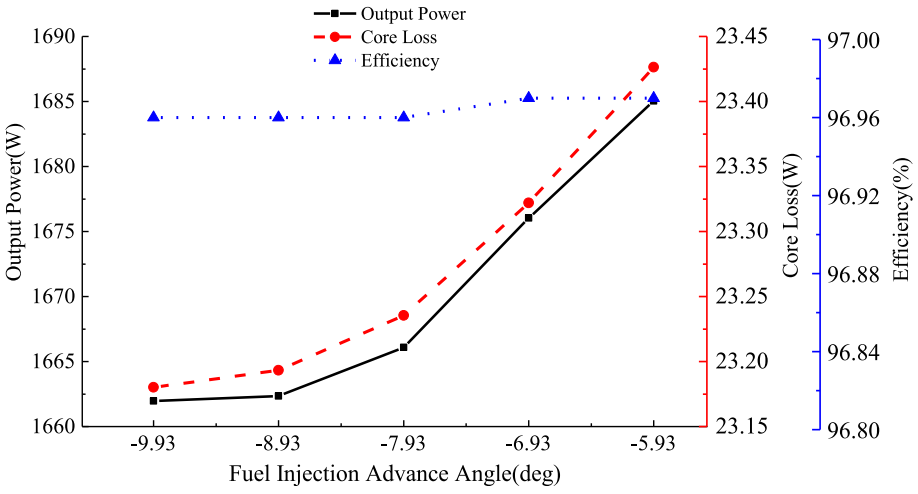

Fig. 17. The influence of injection timing on power, core loss and efficiency of generator.

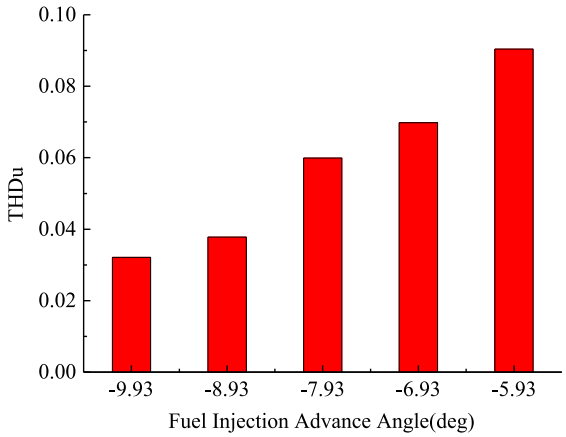

Fig. 18. The influence of injection timing on THDu of generator.

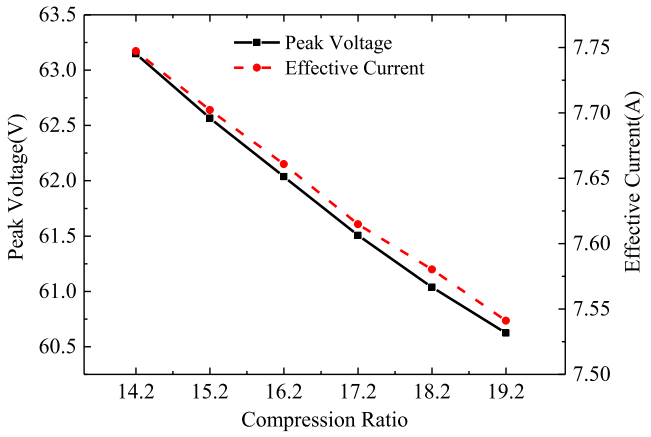

Fig. 20. Variation of peak voltage and effective current with compression ratio.

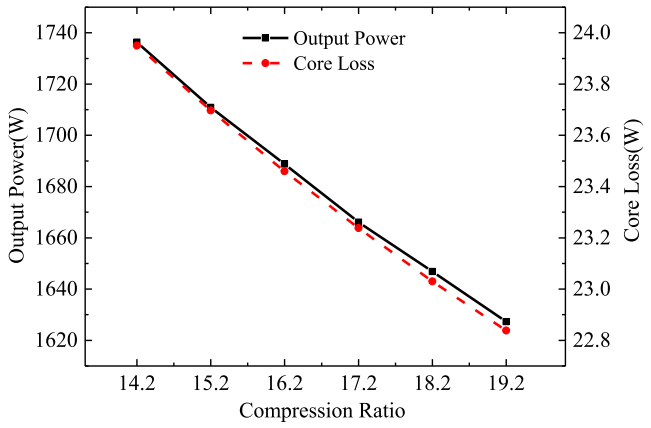

Fig. 21. Variation of power and core loss with compression ratio.

has simple structure, low cost and high system efficiency, which is suitable for vehicle installation.

4. Conclusions

A computational study on using an exhaust power turbine with a high-speed permanent magnet generator to recover the waste heat from the engine exhaust gas has been conducted. A high-speed permanent magnet generator (60,000 r/min) is designed for the purpose. A diesel engine (88 kW at 3600 r/min) is used as the primary mover. Computational models of the engine and the exhaust turbine power generation system are developed using GT-POWER (for the diesel engine), MATLAB/SIMULINK (for the exhaust power turbine) and ANSOFT (for the high-speed permanent magnet generator). Simulation under different conditions and parameters are carried out and the results are shown and discussed above. From this study, the following conclusions can be drawn:

(1) It is possible to use an exhaust power turbine with a high-speed permanent magnet generator to recover the waste heat from the engine exhaust gas to generate electrical power.

(2) The maximum power generated is 1.8 kW at 60,000 rpm. The maximum turbine power obtained is 8.9 kW at 0.18 kg/s mass flow rate. In addition, turbine power increases non-linearly along with the increase in the turbine speed with a maximum value of 7.4 kW at 52,000 rpm. For the 3000 rpm speed, the maximum system efficiency achieved is 42.8%.

(3) As the engine speed increases, the data such as peak voltage, effective current, core loss, power output, THDu and efficiency of generator increases. The maximum output power is 1.9 kW at 3600 rpm. The maximum efficiency obtained is 97.4%. The data of generator increases as the injection timing or compression ratio decreases. The maximum electrical power achieved is 1.7 kW at 14 compression ratio and the maximum efficiency is 97%. In addition, when injection timing is −5 deg, the peak voltage is 62 V, the efficiency is 96.97%, and the maximum obtained power is 1.68 kW.

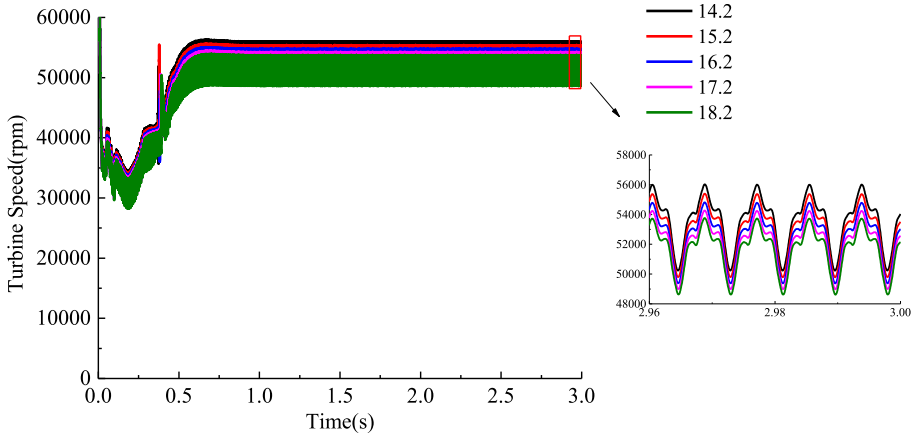

Fig. 19. The power turbine speed with time-variation under different compression ratios.

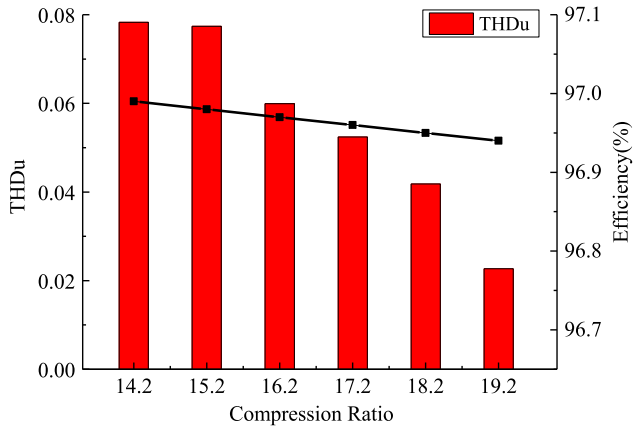

Fig. 22. Variation of efficiency and *THDu* with compression ratio.

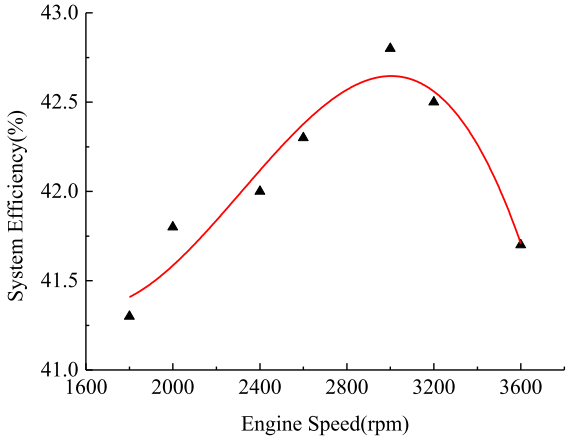

Fig. 23. The system efficiency variation with engine speed.

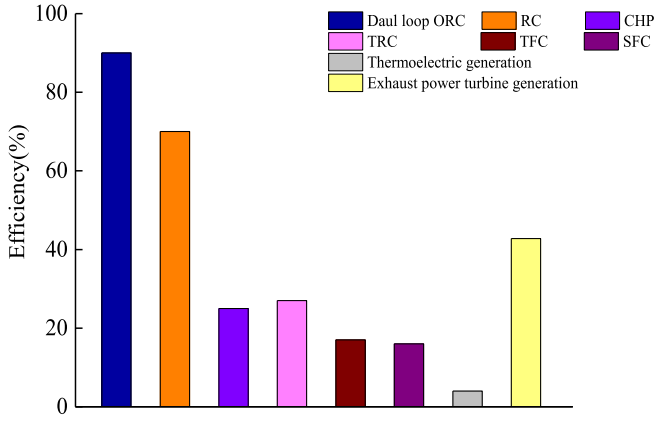

Fig. 24. The system efficiency comparison of waste heat recovery system.

Declaration of competing interest

The authors declare that they have no known competing financial interests or personal relationships that could have appeared to influence the work reported in this paper.

Acknowledgments

This research is supported by the project (52077047) of National Natural Science Foundation of China and (LH2020E092) of Natural Science Foundation of Heilongjiang Province, China.

References

Alshammari, F., Pesyridis, A., et al., 2018. Experimental study of a small scale organic rankine cycle waste heat recovery system for a heavy duty diesel engine with focus on the radial inflow turbine expander performance. Appl. Energy 215, 543–555.

Armstead, J., Miers, S., 2014. Review of waste heat recovery mechanisms for internal combustion engines. J. Ther. Sci. Eng. Appl. 6, 014001–1–014001–9.

Arnaud, L., Ludovic, G., Mouad, D., et al., 2014. Comparison and impact of waste heat recovery technologies on passenger car fuel consumption in a normalized driving cycle. Energies 7, 5273–5290.

Berardi, G., Bianchi, N., 2017. Rotor losses reduction in high speed PM generators for organic rankine cycle systems. In: 2017 IEEE Energy Conversion Congress and Exposition(ECCE), pp. 5396–5402.

Berardi, G., Bianchi, N., 2019. High speed PM generators for organic Rankine cycle systems: Reduction of eddy current rotor losses. IEEE Trans. Ind. Appl. 55 (6), 5800–5808.

Berardi, G., Bianchi, N., Gasperini, D., 2017. A high speed PM generator for an organic rankine cycle system. In: 2017 IEEE International Electric Machines and Drives Conference(IEMDC), pp. 1–8.

Berardi, G., Bianchi, N., Gasperini, D., 2019. A high speed PM generator for an organic Rankine cycle system. IEEE Trans. Ind. Appl. 55 (5), 4633–4642.

Bin Mamat, A., Martinez-Botas, R., 2016. Design methodology of a low pressure turbine for waste heat recovery via electric turbocompounding. Appl. Therm. Eng. 107, 1166–1182.

Dahl, J., 2018. Model predictive control of a diesel engine with turbo compound and exhaust after-treatment constraints. IFAC-PapersOnLine 51 (31), 349–354.

Ekberg, K., Eriksson, L., 2017. Improving fuel economy and acceleration by electric turbocharger control for heavy duty long haulage. IFAC-PapersOnLine 50 (1), 11052–11057.

Giampieria, A., Ling-Chin, J., et al., 2020. A review of the current automotive manufacturing practice from an energy perspective. Appl. Energy 261, 114074.

Gilson, A., Dubas, F., 2016. Comparison of high-speed PM machine topologies for electrically-assisted turbocharger applications. In: 2016 19th International Conference on Electrical Machines and Systems(ICEMS), pp. 1–5.

Gilson, A., Verez, G., Dubas, F., 2017. Design of a high-speed permanent-magnet machine for electrically-assisted turbocharger applications with reduced noise emissions. In: 2017 IEEE International Electric Machines and Drives Conference (IEMDC), pp. 1–6.

He, G., Xie, H., 2017. Investigation into comprehensive fuel saving potential of diesel with electric turbo-compounding waste heat recovery power generation and electric thermal management power consumption system. J. Xi'an Univ. 51 (5), 112–120.

Jung, D., Lee, J., 2018. Design method of an ultrahigh speed PM motor/generator for electric-turbo compounding system. IEEE Trans. Appl. Supercond. 28 (3), 1–4.

Li, J., Xu, Y., Wang, W., 2015b. Study on exhaust energy recycling system of engine. Mach. Des. Manuf. 8, 34–38.

Li, J., Xu, Y., Yu, J., 2015a. Control strategy study on exhaust energy recycling system of engine. Mod. Manuf. Eng. 5, 1–6.

Li, J., Zhu, Y., Xu, Y., 2014. Research on control strategy optimization in power transmission system of hybrid electric vehicle. Mach. Des. Manuf. (3), 138–141.

Lim, M., Kim, J., 2017. Design of an ultra-high-speed permanent-magnet motor for an electric turbocharger considering speed response characteristics. IEEE/ASME Trans. Mechatronics 22 (2), 774–784.

Lin, L., Wang, Y., 2007. An experimental investigation of a household size trigeneration. Appl. Therm. Eng. 27, 576–585.

Liu, J., Fu, J., 2011. A study on the energy flow of diesel engine turbocharged system. J. Hunan. Univ. 38 (5), 48–53.

Nadaf, S., Gangavati, P., 2014. A review on waste heat recovery and utilization from diesel engines. Int. J. Adv. Eng. Technol. 5 (4), 31–39.

Orr, B., Akbarzadeh, A., Mochizuki, M., 2016. A review of car waste heat recovery systems utilising thermoelectric generators and heat pipes. Appl. Therm. Eng. 101, 490–495.

Quinn, R., Dickinson, A., 2005. Tigers Project Overview 2005-06-01.

Rijpkema, J., Munch, K., et al., 2017. Thermodynamic potential of rankine and flash cycles for waste heat recovery in a heavy duty diesel engine. Energy Procedia 129, 746–753.

Romagnoli, A., Vorraro, G., Rajoo, S., 2017. Characterization of a supercharger as boosting & turbo-expansion device in sequential multi-stage systems. Energy Convers. Manage. 136, 127–141.

Shu, G., Liang, Y., 2013. A review of waste heat recovery on two-stroke IC engine aboard ships. Renew. Sustain. Energy Rev. 19, 385–401.

Tang, Q., Fu, J., Liu, J., 2016a. Study of energy-saving potential of electronically controlled turbocharger for internal combustion engine exhaust gas energy recovery. J. Eng. Gas Turbines Power 138 (11), 112805-112805-13.

Tang, Q., Fu, J., Liu, J., 2016b. Comparison and analysis of the effects of various improved turbocharging approaches on gasoline engine transient performances. Appl. Therm. Eng. 93, 797–812.
U.S. Eenergy Information Administration (EIA), 2019. International energy outlook 2019 with projections to 2050, September 2019. https://www,eia.gov/outlooks/ieo/pdf/ieo.
Venkateswarlu, C., Suresh, K., 2018. A technical review on waste heat recovery from compression ignition engines using organic rankine cycle. Renew. Sustain. Energy Rev. 81, 493–509.
Wei, W., Zhuge, W., 2010. Comparative study on electric turbo-compounding systems for gasoline engine exhaust energy recovery. Proc. ASME Turbo Expo 5, 531–539.
Xie, H., He, S., 2016. Optimization of overall efficiency of controllable mechanical heavy duty diesel engines equipped with turbo-compounding system. Chin. Intern. Combust. Engine Eng. 37 (6), 31–36.
Xie, H., Li, S., 2014. Adaptive on driving cycles of waste energy recovery turbo-compound systems on a heavy duty diesel engine. J. Tianjin Univ. 47 (6), 558–564.
Xie, J., Li, X., Li, J., 2017. Design of exhaust energy recovery system controller of hybrid electric vehicle. Modul. Mach. Tool Autom. Manuf. Tech. 10 (10), 96–100.
Xu, Y., 2014. Study of Control Strategy of Hybrid Electric Vehicle Exhaust Energy Recovery System. Chongqing Jiaotong University, Chongqing, pp. 19–22.
Zhang, Y., 2014a. Car exhaust turbine power generation-turbine power determination. Automob. Maint. (10), 4–7.
Zhang, Y., 2014b. EQ6100 type internal combustion engine air consumption calculation. Automob. Appl. Technol. (12), 21–24.
Zhang, Y., 2015a. The study of automotive exhaust gas turbine power generation technology. Small Intern. Combust. Engine Veh. Tech. 6 (44), 53–56.
Zhang, Y., 2015b. Matching vehicle exhaust turbine power generation turbines. Automob. Appl. Technol. (1), 110–113.
Zhao, R., Li, W., 2017. Numerical study on steam injection in a turbocompound diesel engine for waste heat recovery. Appl. Energy 185, 506–518.
Zhao, R., Zhuge, W., Zhang, Y., 2014. Parametric study of power turbine for diesel engine waste heat recovery. Appl. Therm. Eng. 67, 308–319.
Zhao, R., Zhuge, W., Zhang, Y., 2015. Study of two-stage turbine characteristic and its influence on turbo-compound engine performance. Energy Convers. Manage. 95, 414–423.